

Infrared small target detection based on multi-directional cumulative measure

Guofeng Zhang

Xinjiang University

Hongbing Ma (✉ hbma@tsinghua.edu.cn)

Tsinghua University

Askar Hamdulla

Xinjiang University

kurban Ubul

Xinjiang University

Article

Keywords:

Posted Date: April 19th, 2022

DOI: <https://doi.org/10.21203/rs.3.rs-1516917/v1>

License: © ⓘ This work is licensed under a Creative Commons Attribution 4.0 International License.

[Read Full License](#)

Additional Declarations: No competing interests reported.

Infrared small target detection based on multi-directional cumulative measure

Guofeng Zhang^{1,3}, Hongbing Ma^{1,2*}, Askar • Hamdulla¹ and kurban • Ubul¹

¹Xinjiang University, School of Information Science and Engineering, Urumqi 830046, China; fgz@stu.xju.edu.cn;

²Tsinghua University, Beijing National Research Center for Information Science and Technology, Department of Electronic Engineering, Beijing 100084, China;

³Changji Vocational and Technical College, Institute of Information Science and Engineering, Changji, 831100, China;

*corresponding. hbma@tsinghua.edu.cn, Tel.: 18610096522

Abstract

Robustness of small target detection is a researchable hotspot in infrared surveillance system. The residual phenomenon of background clutter is universal in current local comparison methods. Algorithm of sparse low-rank decomposition restoration cannot be applied to the actual situations due to the long time consumption. This letter proposes a multi-directional cumulative measure (MDCM) to enhance saliency and effectiveness of weak-small target detection. Firstly, multi-directional cumulative mean difference is implemented in central layer and background layer to estimate the background, while the multi-directional cumulative derivative multiplying is calculated in central-active layer to characterize overall target's heterogeneity, then technology of image fusion is adopted to eliminate interference of false target. Finally, a simple adjudicative technology is employed toward separated target region from complex scenes. Compared to up to date existing approaches, extensive simulation testing on four public datasets prove that proposed approach is capable of separating small targets efficiently from an irregular background in a single-scale window and achieve a comparable or even better accuracy.

1. Introduction

Technology of infrared small target detection has extensive and realistic significance in infrared search and tracking system, precision guided weapons, infrared surveillance and other fields[1]. Infrared small target detection has always been the vital research content of infrared image processing. Remote small target detection and tracking will be transformed into decision superiority in the future information warfare. Currently, there are two main approaches of target detection at home and abroad: sequential-based and single-frame-based methods[2].

Compared with sequence image detection, single frame detection has fewer restrictions and lower requirements in the field of guidance system. Accordingly, the goal of this letter is to boost detection accuracy of single-frame image and adaptability in engineering field. In recent years, number of researchers are committed to IR small target detection, and put forward variety of single-frame methods in past predecessor achievement foundation, have made outstanding contributions to solve the problem under different conditions. At present, commonly used single-frame IR small target algorithms of detection is roughly capable of separating into methods founded on background suppression, human vision system (HVS) and low-rank and sparse matrix decomposition (LRSMD). Maximum median/mean filtering[3] and morphological top-hat transformation[4] are typical methods based on background

suppression. when the background is homogeneous and simple, these methods are relatively applicable. However in various complex scenes, the performance of filtering degrades rapidly. Approaches based on HVS make use of contrast mechanism in target region and local neighborhood to distinguish target. Typical algorithms such as chen et al.[5] proposed an effective local contrast measure (LCM) with nested filter structure in eight directions, which has a good detection ability and strong anti-interference to enhance the target area. But, LCM amplifies random noise of single pixel, resulting in high intensity clutter of background also produces enhancement in the output image. Therefore, many improved methods based on relative local contrast measure(RLCM)[6], tri-layer local contrast measure(TLLCM)[7] et al. have been proposed. For example, Wei et al.[8] established multi-scale patch contrast measure (MPCM) to detect dark and bright targets by utilizing differences in diagonal background window units. However, some speckled and strong clutter edges similar to the target are still retained after MPCM processing. Madi S et al.[9] proposed absolute directional mean difference (ADMD) and the latest method of an enhanced closest-mean background estimation(ECMBE) proposed by Han et al.[10]. The disadvantage of these methods is that it is difficult to eliminate the clutter with certain prominent high brightness. Especially when target brightness is roughly equal to or lower than background brightness, Leak detection is common. Causing the detect ability cannot meet the requirement in various undulating scene.

The method using LRSMD considers infrared image as the combination of low-rank background matrix and sparse target matrix, the matrix decomposition method originates robust principal component analysis(RPCA)[11] optimization algorithm. Zhao et al. [12] proposed a sparse representation method for infrared small target detection. Gao et al.[13] proposed classic infrared patch-image (IPI) model, which uses sliding windows to acquire sub-images. He et al.[14] introduced low-rank matrix recovery on the basis of sparse representation, and optimized the solution by using the Augmented Lagrange Multiplier (ALM) method, thus improves the robustness and accuracy of detection. Dai et al.[15] proposed a weighted IPI model. Recently, in order to further improve the accuracy of recovering low-rank components, Zhang et al.[16] combined the $l_{2,1}$ norm to describe the background and proposed a novel method based on non-convex rank approximation minimization joint $l_{2,1}$ norm (NRAM). Yao et al.[17] proposed facet kernel and random walker(FKRW). Zhang et al.[18] proposed partial sum of the tensor nuclear norm (PSTNN) method based on infrared patch tensor (IPT) model[19]. Sun et al. [20] used the row sparse norm to replace the kernel norm and did not calculate the singular value of the matrix, which greatly improved speed of the target detection. Yang et al.[21] proposed an ocean target detection approach using significance measure of the target. These methods can achieve good results in the case of high target intensity or relatively obvious contrast. Yet, while background becomes more complex and heterogeneous, or the infrared target becomes small and dim, It is difficult to eliminate the strong edge and sharp noise in the backgrounds, low detection rate and high false positive rate are often unavoidable. In addition, the process of matrix decomposition needs iterative solution, which occupies more computing resources and has poor real-time performance.

In this case, a multi-directional cumulative measure (MDCM) algorithm is proposed to effectively solve this problem, optimization detection performance for IR dim and small targets under complicated backgrounds and efficiently separating small targets in real time. Experimental simulation display that MDCM has better performance in suppressing complex background and enhance the target than some recent algorithms, and achieve a comparable or even better accuracy.

2. The Proposed Methods

Most IR small target detection approaches ignore the directional information. in this fields, on an enhanced closest-mean background estimation (ECMBE) basis, a new multi-directional cumulative mean difference algorithm is constructed in centre-background layer to repress the participation of the

highlighted background. At the same time, a multi-directional cumulative derivative multiplying algorithm is constructed in central-active layer and directional gradient is introduced to enhance potential target. The diagonal derivative multiplying can remarkably enhance target which is stronger than background or weaker than background. Fig.1 exhibits layer structure diagram of the MDCM, and Fig.2 exhibits realization process of the MDCM approach.

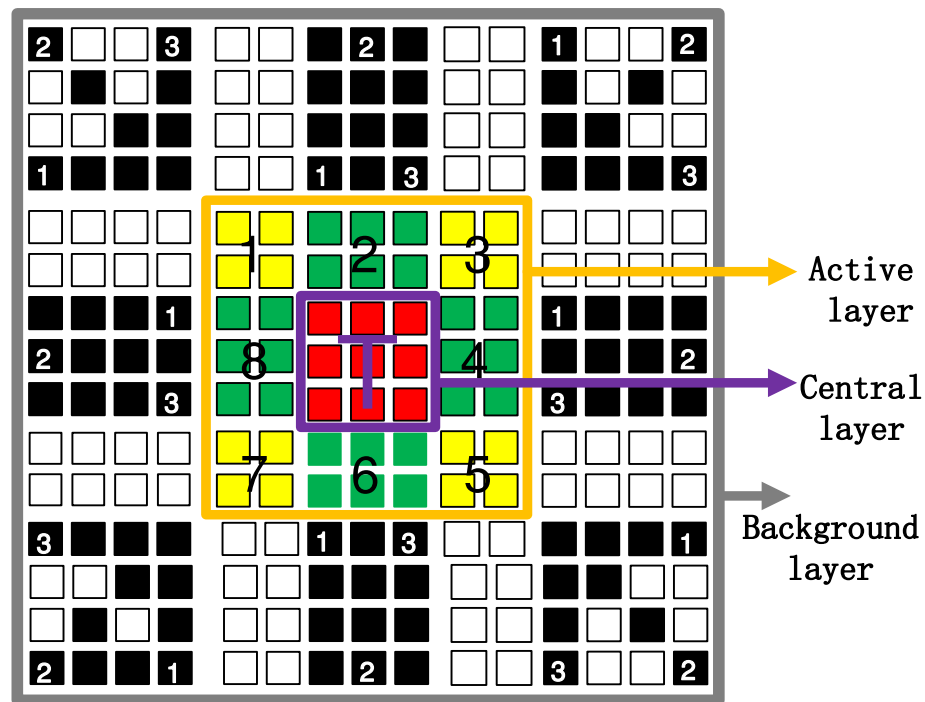


Fig.1. Structure of layered in different directions

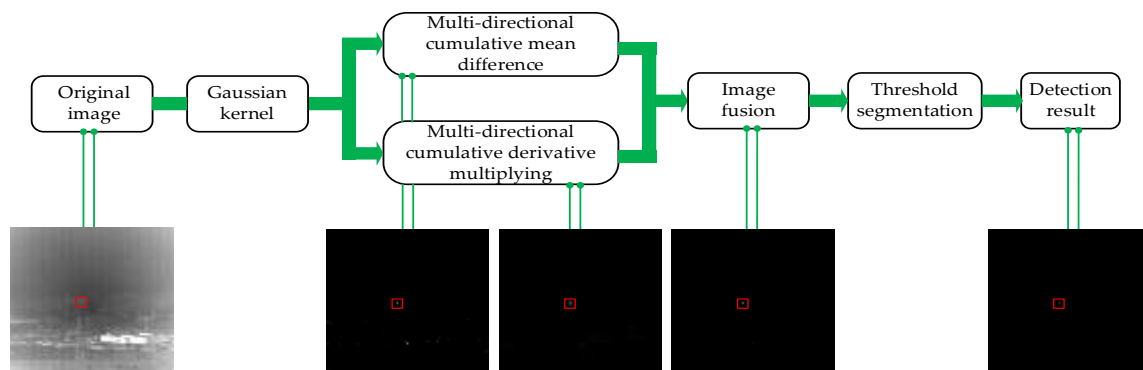


Fig.2. Flow chart of the proposed approach

2.1. Gaussian pre-enhance operation

Infrared small targets have dispersion characteristics from the center to the periphery, diffuse gradient direction of small target is almost comparable in all directions, so true target is closest to the gaussian-like near its center. In a matched filter according to the filter theory, Signal to Noise Ratio(SNR) is capable of improvement best while select filter kernel is identical to shape of signal[22]. So a contrivable normalized

Gaussian Kernel(GK) is employed to raw IR image to pre-enhance target and suppress pixel-like noise high brightness (PNHB). Gaussian Kernel template of the central layer is defined as:

$$G(u, v) = \frac{1}{100} \begin{bmatrix} 7 & 12 & 7 \\ 12 & 20 & 12 \\ 7 & 12 & 7 \end{bmatrix} \quad (1)$$

the pixel of central layer at (i, j) is expressed as:

$$I_c(i, j) = \sum_{u=-1}^1 \sum_{v=-1}^1 I(i+u, j+v) G(u, v) \quad (2)$$

where I represents original input image, G(u,v) represents the GK of equation 1, and I_c(i, j) represents pre-enhance result after gaussian filtering.

2.2. Multi-directional cumulative mean difference

In the background layer, we divide cell window into eight orientation. Average intensity of every cell window can be estimated using pixels in three directions around it. Cell window is mainly employed for the purpose of capturing local neighborhood background pixels as accurately as possible.

For every directions, to accurately estimate the background, cumulative mean gray of in three directions for each sub-cell is proposed in this letter as following.

$$BE_i(x, y) = \frac{1}{3n} \sum_{j=1}^3 \sum_{k=1}^n BL_k^j \quad i = 1, 2, K, 8 \quad (3)$$

where (x, y) represents a coordinate position in the central layer, i is number of sub-cell, BL_k^j represents intensity level of the kth pixel in the jth direction, n represents quantities of pixels in every direction. So as to better restrain interference of highlighted clutter to dim and small targets, the final background estimation(FBE) is calculated using the principle of closest-mean center pixel instead of the max-mean criterion. Multi-directional cumulative mean difference (MDCMD) between center pixel and background pixels in three directions for each sub-cell is defined as:

$$MDCDM(x, y) = \max |I_c(x, y) - FBE(x, y)| \quad (4)$$

$$FBE(x, y) = \arg \min_{BE_i(x, y)} |I_c(x, y) - BE_i(x, y)| \quad (5)$$

2.3. Multi-directional cumulative derivative multiplying

After MDCDM operations, some highlighted background clutter and random noise are still present and residual. Researchers have discovered that the peak value of intensity level of a real target attenuates exponentially with distance[23]. Directional gradients of real small target area are always present and variable in different directions. The gradient coverage of the real target always points roughly to the center of the target area. Fig.3 shows the direction of gradient vector.

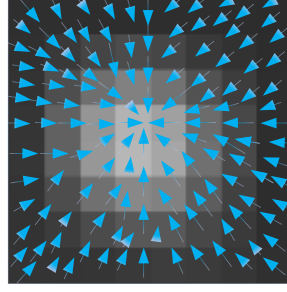


Fig.3. Direction of gradient vector

Maximal size of the small target is up to 9 by 9 pixels, when the window of central pixel moves to the true target center, the active layer is still the larger area where the target energy is concentrated. Multi-directional mean estimation of active layer pixels in three directions for each sub-cell is defined as:

$$D_i = \frac{1}{3n} \sum_{s=1}^3 \sum_{q=1}^n A L_q^s \quad i=1,2,K,8 \quad (6)$$

D_i represents average intensity in the i th sub-cell for active layer, n represents quantities of pixels in every direction. AL_q^s represents intensity lever of the q th pixel in the s th direction, n represents quantities of pixels in every direction. In this letter, to distinguish background edge and true targets, a new variable called directional gradient (DG) threshold is introduced after Multi-directional mean estimation operation.

$$\eta_{DG} = \frac{\max(D_i)}{\min(D_i)} \quad (7)$$

In addition, in order to obtain light or dark targets, calculating the multiplying and difference are applied in active layer.

$$AD_i(x, y) = \min\{A_i, A_{4+i}\} \quad i=1,2,\dots,4 \quad (8)$$

$$A_i(x, y) = I_c - D_i \quad (9)$$

So multi-directional mean cumulative derivative by constraining condition between center layer pixel and active layer pixels in three directions for each sub-cell is defined as:

$$MDMCD(x, y) = \begin{cases} 1 & \text{if } AD_i(x, y) > 100 \text{ and } \eta < 1.5 \\ 0 & \text{otherwise} \end{cases} \quad (10)$$

2.3. Calculation of MDCM

After calculating the MDCMD and MDCDM, The MDCM of one of the pixels in the original infrared input image is calculated by equation 11.

$$MDCM(x, y) = MDCMD(x, y)MDMCD(x, y) \quad (11)$$

The MDCM is calculated for each pixel from left to right and top to bottom pixel by pixel in MDCMD and MDCDM operation. Finally a new saliency map named MDCM is formed.

3. Discussions and Threshold Operation

The results section can include subheadings. When calculating MDCM map in each pixel,next, there are six different pixel types that need to be discussed:

a) If (x, y) is a true target (TT):If the pixel locates the target center, since the target is gaussian-like with a positive local contrast, so its MDCDM and MDMCD are large at the same time. Finally, the result of MDCM is large.

b)If (x, y) locates a pure background area(PB): Pure background always appears as a large and homogeneous area, so there is a small gradient around the pixel in the pure background. Its MDCDM will approximate zero. Therefore, the final MDCM will be much smaller than the target.

c)If (x, y) is a high brightness background(HB):It may have a big intensity level than TT, According to closest-mean center pixel principle, the background estimate is small,MDCMD will is large. However, the directional gradient with the maximum value and minimum value differ greatly in active layer, which probably greater than the gradient threshold, so MDCDM is labeled utmostly as 0.

d)If the pixel is a edge of background (EB):Although the gradient of several MDCMD is still large, the others are kept small. So the value of directional gradient threshold will be large than directional gradient threshold by setting. So MDCDM is calculated as 0. EB could be well restrained.

e)If the pixel is a PNHB:That would probably result in value of AD being less than 0, not participating in the next operation, and MDCDM still is 0.

Though the analysis of the above different situation,massive interference pixels can be further restrained,true target will be evidently prominent and is significantly enhanced after the target saliency map is calculated by MDCM. To thoroughly segment the target from MDCM map, an adaptive decision threshold can be obtained.

$$T = \mu \bullet MDCM_{\max} + (1 - \mu) \overline{MDCM} \quad (12)$$

Where $MDCM_{\max}$ and \overline{MDCM} represent maximum and average values of MDCM map,respectively. μ represents a parameter in the range 0-1.That in the range of the deviation among the parameter μ ,the relation between 0.5 and 0.8 will is more optimal test samples in this article.

4. Experimental Results and Discussions

4.1. Experimental dataset

For sake of proving the reliability of the algorithm under complex background interference.Test examples of four real infrared sequence scenes are shown in Fig.4,Table 1 displays detailed description of the test data. Database of seq.1-3 are derived from the “plane” of thermal image sequences using domestic in a recent public IR datasets[24] and seq.4 is derived from the”plane”of thermal image sequence using a network dataset. we compared proposed model to several recent up to date models with RLCM[6],MPCM[8],TLLCM[7],FKRM[17],PSTNN[18],NRAM[16] and ECMBE[10].The parameter settings of all the compared methods are consistent with the authors’suggestions. The simulations are implemented in MATLAB 2016b software on the same computer with an intel 3.20 GHz dual-core i5-4460 CPU, NVIDIA GeForce GTX1050Ti and 8GB RAM. Fig.4.presents the qualitative comparison results using proposed method and up to date approaches.The first column demonstrates representative frames of every raw scene, columns 2-9 are compared results,namely RLCM[6],MPCM[8],TLLCM[7],FKRM[17],PSTNN[18],NRAM[16],ECMBE[10] and proposed method.

Table 1. Detailed description of test datasets

	Frames	Size	Target Size	Target number	Target type	Background type
Seq.1	400	256×256	2×3	1	unmanned aerial vehicle	Background of ground with varying degrees of thermal noise
Seq.2	400	256×256	3×3	1	unmanned aerial vehicle	Background of sky-ground
Seq.3	400	256×256	1×2	1	unmanned aerial vehicle	Complex ground background with banded highlighted interference.
Seq.4	200	256×256	3×5	1	unmanned aerial vehicle	Background with heavy floccus cloud.

4.2. Qualitative evaluation

In seq.1, all the methods are capable of detecting small target, especially NRAM and the proposed algorithm can not only enhance the target significantly, but also are extraordinary superior in suppressing the highlight background clutter. RLCM,MPCM,TLLCM and ECMBE all contain tiny amounts of clutter with pixel size, RLCM has also better enhanced performance to target area,MPCM,TLLCM and ECMBE have high brightness noise points at some regions, threshold separation is likely to fail to eliminate false targets. FKRM and PSTNN significantly have patches of speckled clutter,this is due to the influence of continuous highlight buildings under the ground background, the background suppression ability is relatively weak. In seq.2,clutter suppression ability of TLLCM and NRAM is also superior, the target protrudes obviously, but there are some dark and faint noise points.The proposed algorithm also has strong anti-clutter performance,and performance of target enhancement is more obvious in spite of existing dark noise points. Threshold separation can eliminate false noise points. RLCM has more speckled clutter and poor anti-interference ability. The clutter brightness in MPCM and FKRM is almost equal to the target region brightness. PSTNN and ECMBE have limited capacity of clutter suppression in background edge region, and there are flaky highlighting and edge linear spot interference.Threshold separation is difficult to eliminate false targets. In seq.3, the target enhancement of the proposed algorithm is very prominent under banded highlighted interference, which is due to the diagonal product principle proposed for dark target detection (Equation 8). The targets detected by NRAM are very weak, and threshold separation is likely to filter out small targets, resulting in leak detection. The targets detected by TLLCM, FKRM and PSTNN are extremely weak, clutter completely submerges the targets, and threshold separations are impossible to extract small targets. RLCM,MPCM and ECMBE cannot detect real targets. In seq.4, the proposed algorithm has excellent ability whether in enhancing target or clutter suppression.In NRAM, the brightness of the interfering pixels is slightly lower than the target.This is not conducive to threshold separation. ECMBE has more noise point interference with high brightness which is difficult for target extraction. MPCM, TLLCM, FKRM and PSTNN are relatively good for background suppression, and the target is also prominent. RLCM has more clutter points and enlarges the target area. All in all, in different scenarios the target processed by MDCM shows strong robustness to target enhancement and background suppression, which is more salient or exceeds all comparison methods.

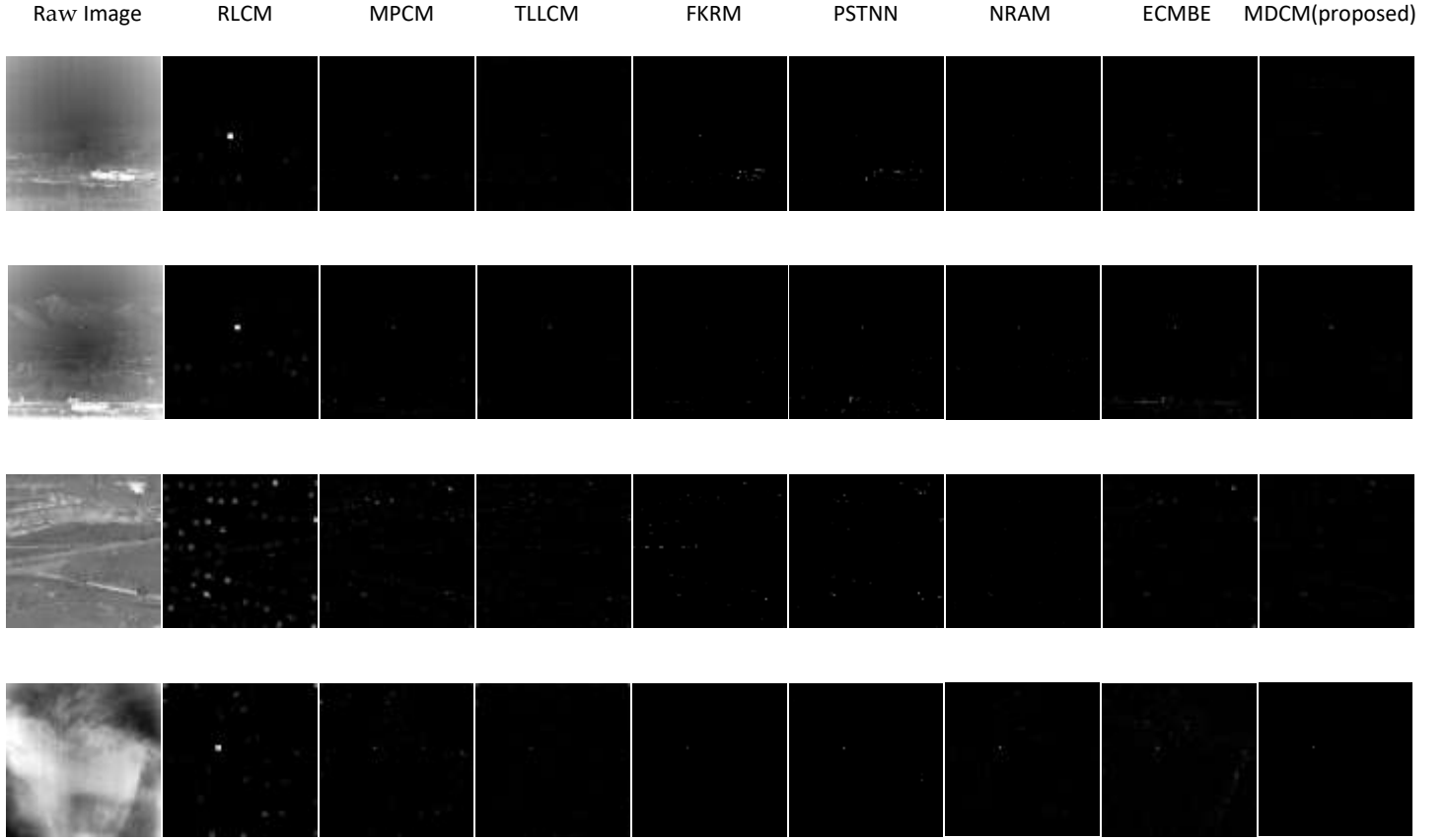


Fig. 4. Original example scenarios with corresponding enhanced maps in different algorithm

4.3. Quantitative evaluation

In quantitative evaluation, BSF and SCRG indicators are specially used to evaluate the algorithm's ability to restrain background clutter and enhanced target signal. The higher the value of the two, the better the performance of the algorithm.

$$BSF = \frac{\sigma_{in}}{\sigma_{out}} \quad (13)$$

$$SCRG = \frac{SCR_{out}}{SCR_{in}} \quad (14)$$

where σ_{in} and σ_{out} represent standard deviation of raw input image and corresponding enhanced map, respectively. SCR_{in} and SCR_{out} represent signal to clutter ratio (SCR) of the raw input image and corresponding enhanced map, respectively.

Table 2. BSF and SCRG of different algorithms

	seq.	RLCM	MPCM	TLLCM	FKRM	PSTNN	NRAM	ECMBE	Proposed
BSF	1	15.7124	17.4571	56.0427	6.2145	90.5876	96.5847	69.8454	130.7451
	2	12.3162	7.2554	124.5121	14.8746	18.2545	102.6254	164.2157	210.2845
	3	1.2139	2.1204	1.0215	0.9847	9.6621	24.3215	17.5820	18.8234
	4	3.5213	13.2065	2.6854	4.5287	32.1874	31.5940	24.8424	69.2547
SCRG	1	36.2754	47.2055	81.9425	20.5142	190.5421	157.6581	184.6584	241.6852
	2	25.6497	16.7524	25.1587	22.6624	170.6825	162.8544	102.5863	161.5486
	3	1.5423	0.9845	2.6231	1.6995	67.4853	49.0814	19.5874	154.2156
	4	10.3542	21.4571	6.8641	13.5748	94.8361	75.9426	62.5866	140.5684

Table 2 shows value of BSF and SCRG, it can be seen that criteria of proposed algorithm are obviously higher than comparative algorithms simultaneously no matter in ground background, sky-ground or heavy floccus cloud background. The higher value of the two index, the better the method performance compared to other state-of-the-art approaches. Even though in more complex scenario 3, the small target is completely submerged, the proposed model acquires a great advancement comprehensively compared with the up to date algorithm in both criterias of BSF and SCRG. Comparative approaches couldn't attain a great BSF as well as SCRG at the same time. Bold datas represent the maximum in table 2. From what has been discussed above, we may safely draw the conclusion that proposed model can advance the saliency of the targets and suppress the complicated backgrounds remarkably.

In Fig.5, Receiver operating characteristic(ROC) curve is introduced to assess the performance of the model to predict detection outcome, it describe a relation among probability of detection (P_d) with false alarm rate (F_a) as judgment in each whole sequence. They are respectively defined as:

$$P_d = \frac{\text{number of detected true targets}}{\text{total number of true targets}} \times 100\% \quad (15)$$

$$F_a = \frac{\text{number of detected false targets}}{\text{total number of pixels in tested frames}} \times 100\% \quad (16)$$

Figure 5 shows that the area of ROC curve of the proposed algorithm is larger than other comparison algorithms. On same false alarm probability, the detection rates are higher under four different scenarios. Especially when the targets suffer from banded highlighted interference clutters in seq.3, the detection rate can reach to 94.7%, and NRAM also achieves a high detection rate, however it is slightly worse than the proposed algorithm. Other algorithms are not robust and the detection rate is unstable. From the perspective of quantitative indicators, our algorithm basically tends to be consistent, reaching the level of similar or much higher than similar comparison algorithms, showing strong anti-interference ability against different backgrounds as a whole, and achieving the balance of detection rate.

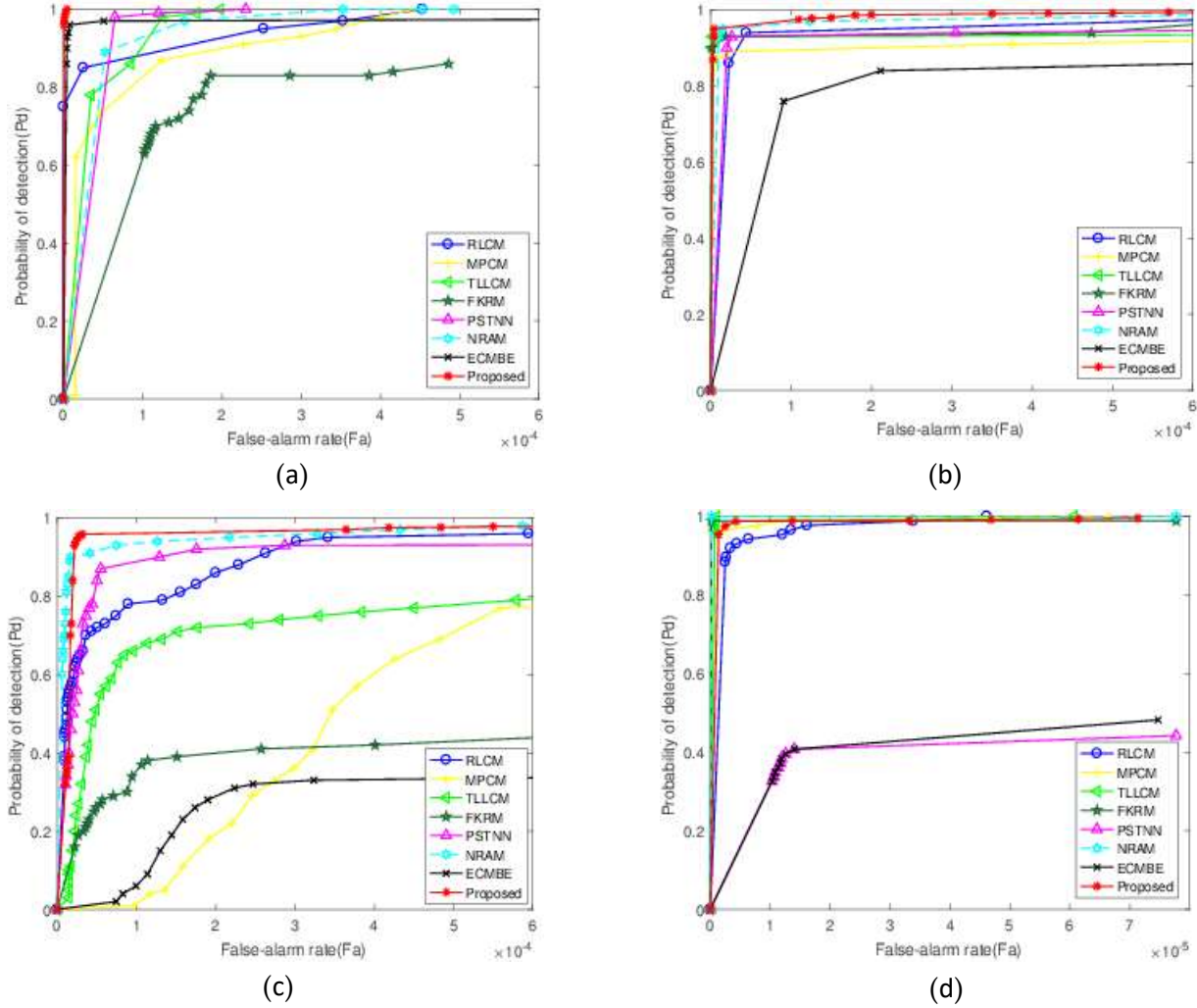


Fig. 5. ROC curves of data set 1-4.

5. Conclusions

This letter proposed an IR small target detection approach derived from multi-directional cumulative mean difference measurement. First, an application of typical gaussian filter kernel for the central layer improves SNR of image. Next in the background layer a closest-mean principle with multi-directional cumulative mean difference is proposed to utmostly estimate the background. Meanwhile, using of multi-directional cumulative derivative multiplying suppress background clutters with sharp edge, in active layer, directional gradient proposed eliminates random noise. Then, The fusion of MDCMD and MDCDM further suppressed the background clutter and enhanced the target region. Finally, an adaptive decision threshold is applied for the sake of achieving target region. The single-scale detection algorithm greatly reduces the complexity of computation instead of using multi-scale windows. Extensive simulated experiments using public IR datasets demonstrate the saliency and robustness of proposed algorithm in irregular and complicated types of background clutter. The performance analysis compared with other algorithm demonstrates the proposed algorithm can efficiently suppress the sensitivity of clutter interfere and achieve a comparable and robust accuracy.

Funding: This research was funded by Shanghai Aerospace Science and Technology Innovation Fund under Grant No. SAST2019-048.

Funding: This research was funded by Cross-Media Intelligent Technology Project of Beijing National Research Center for Information Science and Technology (BNRist) under Grant No. BNR2019TD01022.

Funding: This research was funded by National Natural Science Foundation of China, grant number 61563049.

Funding: This work was supported by the National Natural Science Foundation of China, grant number (No.61862061,61563052,61163028).

Data availability

The datasets generated and/or analysed during the current study are not publicly available due [REASON WHY DATA ARE NOT PUBLIC] but are available from the corresponding author on reasonable request.

References

1. Y. Chen, B. Song, D. Wang, and L. Guo, "An effective infrared small target detection method based on the human visual attention," *Infr. Phys. Technol.*, vol. 95, pp. 128–135, Dec. 2018.
2. C. Q. Gao, D. Meng, Y. Yang, Y. Wang, X. Zhou, and A. G. Hauptmann, "Infrared patch-image model for small target detection in a single image," *IEEE Trans. Image Process.*, vol. 22, no. 12, pp. 4996–5009, Dec. 2013.
3. S. Deshpande, M. Er, and R. Venkateswarlu, "Max-mean and max-median 7-filters for detection of small-targets," in *Proc. SPIE*, Oct. 1999, vol. 3809, pp. 74–83.
4. V. Tom, T. Peli, M. Leung, and J. Bondaryk, "Morphology-based algorithm for point target detection in infrared back-grounds," in *Proc. SPIE*, Oct. 1993, vol. 1954, pp. 2–11.
5. C. P. Chen, H. Li, Y. Wei, T. Xia, and Y. Y. Tang, "A local contrast method for small infrared target detection," *IEEE Transactions on Geoscience and Remote Sensing*, vol. 52, no. 1, pp. 574–581, 2013.
6. J. Han, K. Liang, B. Zhou, X. Zhu, J. Zhao, and L. Zhao, "Infrared small target detection utilizing the multi-scale relative local contrast measure," *IEEE Geosci. Remote Sens. Lett.*, vol. 15, no. 4, pp. 612–616, Apr. 2018.
7. J. Han, S. Moradi and I. Faramarzi, "A Local Contrast Method for Infrared Small-Target Detection Utilizing a Tri-Layer Window," *IEEE Geosci. Remote Sens. Lett.*, vol. 17, no. 10, pp. 1822–1826, Apr. 2020.
8. Y. Wei, X. You, and H. Li, "Multiscale patch-based contrast measure for small infrared target detection," *Pattern Recognit.*, vol. 58, pp. 216–226, Oct. 2016.
9. Moradi S, Moallem P, Sabahi M F. "Fast and robust small infrared target detection using absolute directional mean difference algorithm," *ScienceDirect[J]. Signal Processing*, 177.
10. J. Han, C. Y. Liu and Y. C. Liu, "Infrared Small Target Detection Utilizing the Enhanced Closest-Mean Background Estimation," *IEEE J Sel. Top. Appl. Earth Obs. Remote Sens.*, vol. 14, pp. 645–662, Jan. 2021.
11. Lin, Z.; Chen, M.; Ma, Y." The Augmented Lagrange Multiplier Method for Exact Recovery of Corrupted Low-Rank Matrices," *arXiv*, 2010; arXiv:1009.5055v3.
12. J. Zhao, Z. Tang, J. Yang, and E. Liu, "Infrared small target detection using sparse representation," *Journal of Systems Engineering and Electronics*, vol. 22, no. 6, pp. 897–904, 2011.
13. C. Gao, D. Meng, Y. Yang, Y. Wang, X. Zhou, and A. G. Hauptmann, "Infrared patch-image model for small target detection in a single image," *IEEE Transactions on Image Processing*, vol. 22, no. 12, pp. 4996–5009, 2013.
14. Y. J. He, M. Li, J. L. Zhang, and Q. An, "Small infrared target detection based on low-rank and sparse representation," *Infra-red Physics Technology*, vol. 68, pp. 98–109, 2015.

- 15.Y. D. A, Y. W. A. B. C. D, and Y. S. A, “Infrared small target and background separation via column-wise weighted robust principal component analysis,” *Infrared Physics Technology*, vol. 77, pp. 421-430, 2016.
- 16.L.Zhang,L.Peng, T.Zhang, S.Cao, Z.Peng.” Infrared small target detection via non-convex rank approximation minimization joint l_2, l_1 norm,” *Remote Sensing*, vol. 10, no. 11, 2018.
- 17.Q.Yao , L.Bruzzone, C.Gao, et al. “Infrared Small Target Detection Based on Facet Kernel and Random Walker,”*IEEE trans-actions on geoscience and remote sensing : a publication of the IEEE Geoscience and Remote Sensing Society*, 2019, 57(9):7104-7118.
- 18.L.Zhang,L.Peng,”Infrared Small Target Detection Based on Partial Sum of the Tensor Nuclear Norm,” *Remote Sensing*, 2019, 11(4):382.
- 19.Y. M. Dai and Y. Q. Wu, “Reweighted infrared patch-tensor model with both nonlocal and local priors for single-frame small target detection,”*IEEE J. Sel. Top. Appl. Earth Obs. Remote Sens.*, vol. 10, no. 8, pp. 3752-3767, Jul. 2017.
- 20.S. Dawei, R. Changjun, X. Dong, G. Ming, Q. Ruixue, and Y. Dongfang,“Joint row and half-norm sparse representation al-gorithm for infrared small target detection,” *Journal of Chinese Inertial Technology*, 2019.
- 21.P. Yang, L. Dong, and W. Xu, “Infrared small maritime target detection based on integrated target saliency measure,” *IEEE Journal of Selected Topics in Applied Earth Observations and Remote Sensing*, vol. PP,no. 99, pp. 1–1, 2021.
- 22.Hermand J P , Roderick W I . Acoustic model-based matched filter processing for fading time-dispersive ocean channels: theory and experiment[J]. *IEEE Journal of Oceanic Engineering*, 1993, 18(4):447-465.
- 23.Hong Z , Lei Z , Ding Y , et al. Infrared small target detection based on local intensity and gradient properties[J]. *Infrared Physics & Technology*, 2017, 89:88-96.
- 24.Bing.H,Zhi.S,Hong.F,et al. dim and small aircraft target detection and tracking dataset in radar echo sequence [DB/OL].*Science Data Bank*, 2019. (2019-10-29). DOI: 10.11922/sciencedb.908.

Competing interests (mandatory)

the authors declare no competing interests).